Progress in total reflection X-ray fluorescence spectrometry at Raja Ramanna Centre for Advanced Technology

M. K. Tiwari[1,*], G. S. Lodha[1], K. J. S. Sawhney[2], B. Gowrisankar[1], A. K. Singh[1], G. M. Bhalerao[1], A. K. Sinha[1], Arijeet Das[1], A. Verma[1] and R. V. Nandedkar[1]

[1]Indus Synchrotron Utilisation Division, Raja Ramanna Centre for Advanced Technology, Indore 452 013, India
[2]Diamond Light Source Ltd, Chilton, Didcot, OX11 0DE, UK

Total reflection X-ray fluorescence (TXRF) spectroscopy has attracted interest in recent years. Using this technique, almost all elements ranging from sodium ($Z = 11$) to uranium ($Z = 92$) in the periodic table can be detected and analysed in a wide concentration range in a single measurement. The present state-of-the-art sensitivities of TXRF are stretched to femtogram range by employing synchrotron radiation as an excitation source. This article aims to provide a basic overview of the TXRF technique to the general readers. We describe a TXRF spectrometer developed in a laboratory source. An X-ray fluorescence-microprobe beamline for TXRF is being constructed, as an extension of this activity, on the Indian synchrotron source, Indus-2.

Keywords: Multilayer thin films, standing wave, X-ray fluorescence spectrometry.

X-RAY fluorescence (XRF) spectrometry is a well-established technique for elemental analysis at the micro and trace level. This technique finds several applications in a variety of fields[1–5]. The technique is mostly non-destructive in nature and has sensitivities in parts per million (ppm) level in relative concentration or microgram of absolute mass. Variation of XRF has continuously evolved either in the form of conventional energy dispersive X-ray fluorescence (EDXRF) or wavelength dispersive X-ray fluorescence (WDXRF) techniques. Figure 1 provides the schematic for EDXRF and WDXRF techniques. In EDXRF (Figure 1 *a*), the dispersion and detection of fluorescence photons are performed using a solid state X-ray detector and a multichannel pulse height (MCA) analyser. This produces an accumulating digital spectrum that can be processed further to derive the concentration of different elements present in a sample. On the other hand, in WDXRF (Figure 1 *b*), the emitted fluorescence X-rays from a sample are separated by Bragg diffraction using a crystal monochromator before being detected. The EDXRF technique has an advantage over WDXRF, that it does not contain any moving mechanical components. Moreover, it provides fast and simultaneous multielement analysis for a sample. Nevertheless, the technique suffers from a serious disadvantage of inferior energy resolution compared to the WDXRF method.

Total reflection X-ray fluorescence (TXRF) spectrometry is one of the variations of the EDXRF method[6] in which: (i) the specimen is excited by the primary X-ray beam at a glancing angle less than the critical angle at which total external reflection occurs, and (ii) primary exciting radiation is incident on a plane polished surface, which serves either as a sample support or is itself the object to be examined. This mode of excitation almost completely eliminates the large Compton scattering of the primary X-ray beam from the sample bulk, which usually limits the detection sensitivities in the conventional EDXRF method. The reduced Compton scattering in TXRF mode as well as enhancement of analyte fluorescence intensity due to twofold excitation during incident and reflected beams results in improved elemental detection sensitivities at few part per billion (ppb) level.

Now-a-days, from the application point of view, TXRF spectrometry has become quite popular in semiconductor industry for analysing trace and ultra-trace elemental impurities in semiconductor devices and wafers, introduced during manufacture procedure. Several synchrotron radiation-based TXRF facilities have been built in recent years at several synchrotron sources worldwide, for industrial utilization of the technique in semiconductor technology[7].

In addition to trace elemental analysis, the TXRF technique finds applications for surface and near-surface layer characterization. The grazing incidence X-ray fluorescence (GIXRF) technique has the potential of being one of the most powerful and versatile methods for characterization of layered materials, because it combines features of both X-ray reflectivity and X-ray fluorescence. GIXRF enables the non-destructive determination of layer thickness, density, interface roughness and depth profiling for an element inside a layer structure.

Considering the various attractive features of the TXRF technique and its applicability to diverse fields, we have designed and developed a simple and versatile TXRF spectrometer in our laboratory[8,9]. This spectrometer allows

*For correspondence. (e-mail: mktiwari@cat.ernet.in)

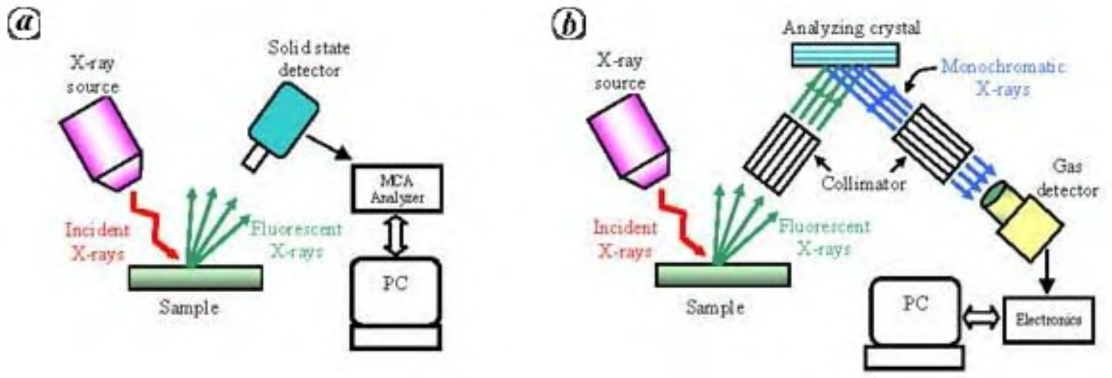

Figure 1. Schematic layout of (*a*) EDXRF and (*b*) WDXRF techniques.

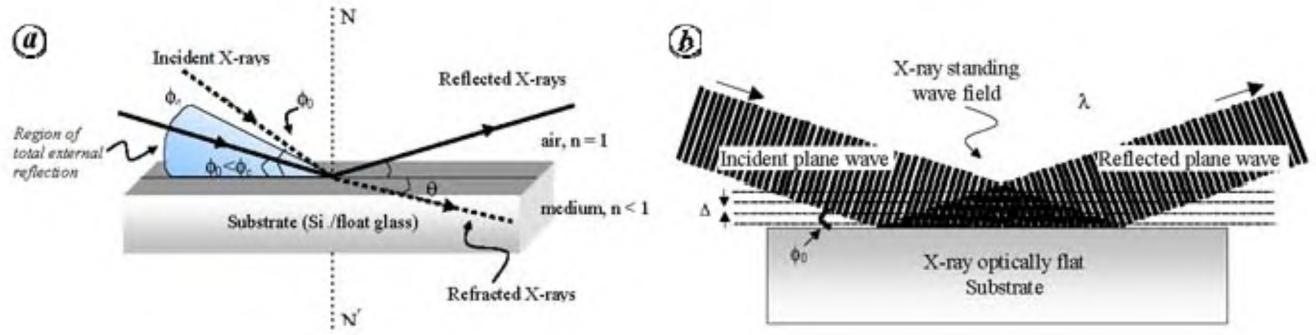

Figure 2. ***a***, Reflection and refraction of X-rays on a flat surface. ϕ_0 and θ are the angles of incidence and refraction respectively, defined with respect to the sample surface. ***b***, The super position of two plane waves on a reflector surface under total external reflection condition generates an XSW field of periodicity $\Delta = \lambda \sin\phi_0$ for incidence angles ($0 < \phi_0 < \phi_c$). The interference fringe generated, are planes parallel to the surface. Maximum intensity of a bright fringe can be achieved as high as about four times the incident intensity.

one to perform ultra-trace elemental analyses as well as thin film and surface characterization. The performance of the TXRF spectrometer developed and a few examples of applications for which it has been used are briefly described in this article. We also describe a microprobe XRF facility which is being constructed on the Indus-2 Indian synchrotron source. The microprobe XRF mode would help in investigating the elemental heterogeneity present in any specimen at micron spatial resolution.

Theoretical background

For X-rays, the complex refractive index $\tilde{n}$ of all materials is slightly less than unity and is given by

$$\tilde{n} = 1 - \delta - i\beta,$$

where δ is a decrement term which describes the deviation of the real part of $\tilde{n}$ from unity, while β denotes the absorption of X-rays into the medium.

If ϕ_c is the critical angle of incidence (Figure 2 *a*), then it can be shown in good approximation that

$$\sin\phi_c \sim \sqrt{2\delta}.$$

The value of δ is usually small and in the range 10^{-3}–10^{-6} for most of the materials. This implies that the total external reflection of X-rays takes place at extreme grazing incidence angles. For example, for quartz or silicon substrate, the critical angle is less than 4 mrad (~0.21°) for Cu-K_α X-ray energy (~8.05 keV).

In the TXRF condition, an X-ray standing wave (XSW) field occurs in a triangular section above the surface, where the incoming and reflected beams cross each other (Figure 2 *b*). This XSW field is generated as a result of interference of incident and reflected beams. The period of the XSW field is given by[6]:

$$\Delta = \frac{\lambda}{2\sin\phi_0} \quad [\text{for } 0 < \phi_0 < \phi_c].$$

For small values of ϕ_0 ($<<\phi_c$), the phase shift between the incident and the reflected X-ray beam would be ~180°. In this condition, the node of the X-ray standing wave field coincides at the surface of the substrate. At the critical angle, the phase shift is close to zero and an antinode is formed near the surface. The node to antinode distance and their position with respect to the surface of the substrate can be changed by changing the incidence angle from zero to the critical angle. It is possible to use this

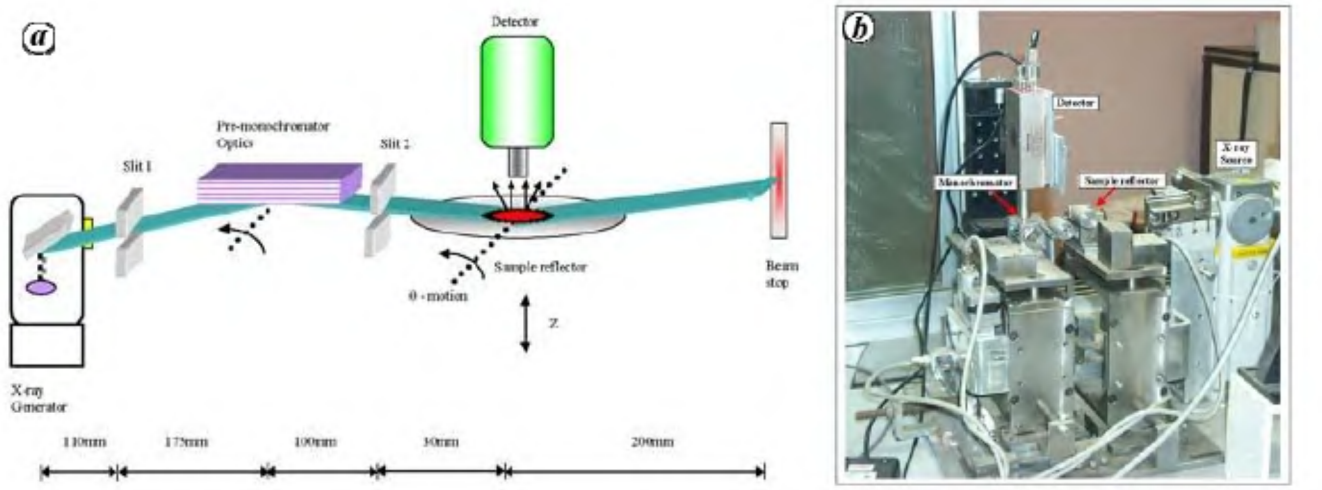

Figure 3. ***a***, Schematic arrangement of the TXRF set-up developed at RRCAT. ***b***, Photograph of the TXRF spectrometer.

XSW field as a probe to find out the location of an impurity atom near the surface. One observes the fluorescence intensity from an impurity atom excited by the XSW field as a monitor of the location. The fluorescence intensity will be larger when the position of an impurity atom coincides with that an antinode. A low fluorescence signal is observed if the node of the XSW field coincides with the position of the impurity atom. Beyond the critical angle, the reflected intensity becomes weak, thereby decreasing the contrast of the XSW field on the flat surface and only a small modulation in the fluorescence intensity is observed. In this condition, the fluorescence excitation is mainly performed by the primary incident beam.

Experimental

Figure 3 *a* shows a schematic layout of the TXRF spectrometer, while Figure 3 *b* shows the photograph of the spectrometer developed at the Raja Ramanna Centre for Advanced Technology (RRCAT), Indore. Most of the components of the TXRF spectrometer have been designed and fabricated in-house. It essentially comprises of an X-ray generator, a slit-collimator attachment, a monochromator stage (i.e. first reflector), a sample reflector stage (i.e. second reflector) and an X-ray detection system. The mechanical details of the spectrometer are described elsewhere[8]. As a monochromator, we have employed a Ni/C multilayer monochromator [$d = 7.0$ nm, $\Gamma = 0.47$, $N = 30$] fabricated in-house. It provides well-resolved Cu-K_α (8.05 keV) radiation of bandwidth ~400 eV for excitation. The detection system for energy-dispersive measurements consists of a Peltier-cooled solid-state detector, a spectroscopy amplifier AMP-6300 and a multichannel pulse height analyser installed on a personal computer. The solid-state detector provides an energy resolution of ~170 eV at 5.9 keV and operates without liquid nitrogen.

The effect of total external reflection of X-rays on the elemental detection sensitivity is demonstrated in Figure 4, wherein the fluorescence spectra recorded from a 100 ng aqueous residue of Fe, deposited on a float glass, are shown for two excitation geometries: (i) non-TXRF mode and (ii) TXRF mode. For the two modes, the grazing angles of incidence are set to 0.12° and 0.07° that are respectively above and below the critical angle of the float glass substrate, which is ~0.1° for Mo-K_α (17.4 keV) X-ray energy. It can be seen from Figure 4 *a* that in the non-TXRF mode, a large Ca-K_α fluorescence signal from the glass substrate as well as large spectral background are present because of the deep penetration of the primary X-ray beam into the substrate material. On the other hand, in the total reflection mode (Figure 4 *b*), the primary beam does not penetrate into the float glass substrate, except a minimum penetration depth and thus only the specimen residue deposited on top of the glass surface gets excited. This results in a substantial reduction of Ca-K_α fluorescence intensity and the spectral background. Furthermore, the fluorescence intensity of the analyte (Fe) gets enhanced because, in addition to the primary beam the reflected beam also excites the fluorescence of the analyte. Both these conditions help to drastically improve the signal-to-noise ratio thereby improving the detection sensitivities achieved for TXRF to one order of magnitude higher or more compared to the non-TXRF mode. We have determined the elemental detection sensitivities for various elements with the TXRF spectrometer (Figure 5). Various single-element liquid standards of concentration 10 µg/ml were prepared from GR-grade chemicals by mixing in de-mineralized water. Then 5–10 µl volume of these solutions was pipetted onto a sample carrier (float glass) using a micropipette and dried by slow evaporation. The residues left on the glass substrate were then analysed using the TXRF spectrometer. Measurements were performed using a Cu target X-ray tube operated at

40 kV, 25 mA and each spectrum was measured for an acquisition time of 1000 s. Figure 5 shows that the detection sensitivities are in the range 2–100 pg for elements Ca to U.

Grazing incidence X-ray fluorescence analysis

The angular dependence of TXRF, also known as GIXRF analysis, was for the first time demonstrated by Becker *et al.*[10]. In the GIXRF method, an angle-dependent X-ray fluorescence profile is recorded for a range of shallow grazing incidence angles (for instance, 0° to 2° in steps of 0.005° or less). de Boer[11] presented a detailed theoretical treatment for the model calculation of GIXRF intensity from a layered material. It has been demonstrated that by changing the glancing incidence angle, the depth sensitivity in layered materials can be enlarged into nanometer region. We have employed our TXRF spectrometer for a variety of GIXRF applications, including surface characterization, thin film analysis and XSW measurements[12–14]. A computer program 'CATGIXRF' has been developed for GIXRF characterization of layered materials[15]. A few examples of GIXRF applications undertaken using our TXRF spectrometer are given here.

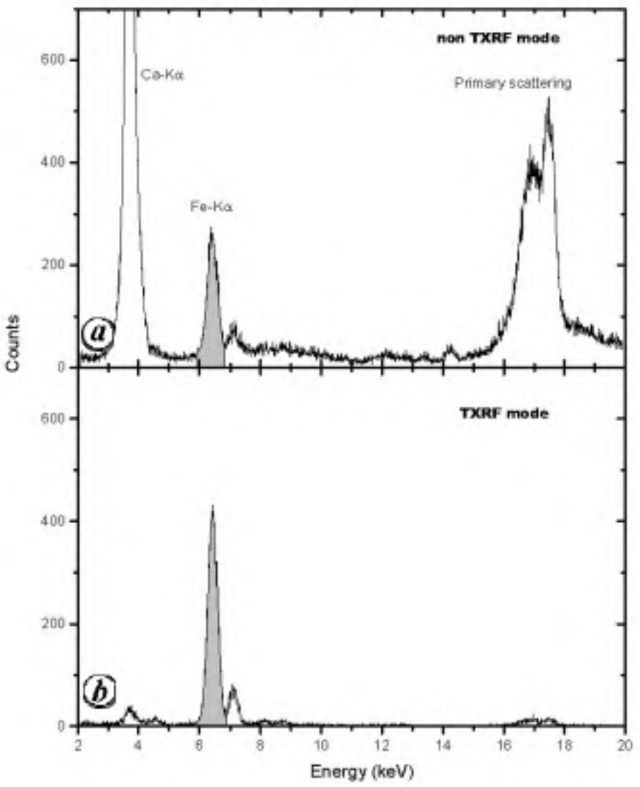

Figure 4. X-ray fluorescence spectra recorded in two excitation geometries (Mo X-ray tube, 35 kV, 10 mA, 50 s). ***a***, Non-TXRF mode: Incidence angle has been set above the critical angle. ***b***, TXRF mode: Incidence angle has been set below the critical angle.

Nanoparticles characterization

The angle-dependent X-ray fluorescence intensity in the TXRF region is capable of distinguishing various types of contamination on a substrate surface[16,17]. The contaminations are broadly identified as bulk type, particulate type and thin layer type. We have demonstrated that if an impurity is present in the form of nanoparticles on top of a Si substrate surface, it can be analysed by the TXRF technique[18]. It is possible to determine average vertical height of the nanoparticles. One can also evaluate whether the distribution of the nanoparticles on the substrate surface exhibits monodispersion or form agglomerations. Figure 6 shows the recorded GIXRF profiles for different forms of Fe particles on top of a Si substrate. In Figure 6 *a*, the measured GIXRF profile for Fe droplet residue particles is shown. Figure 6 *b* and *c* shows the measured GIXRF profiles in the case of monodispersed nanoparticles and agglomerated nanoparticles respectively, on a Si substrate. The GIXRF measurements (Figure 6 *b*) gives the average vertical heights of Fe nanoparticles as ~31 nm, which has been confirmed independently using atomic force microscopy and scanning electron microscopy (SEM) measurements. The insets in Figure 6 show the SEM pictures for the respective cases. From Figure 6 *c*, it can be seen that the GIXRF profile changes remarkably as the agglomerations of nanoparticles takes place on the Si substrate surface. In this condition one obtains the GIXRF profile of Fe nanoparticles similar to Fe droplet residue particles.

Thin film characterization

One of the most common applications of the GIXRF is the characterization of thin film structures. In Figure 7,

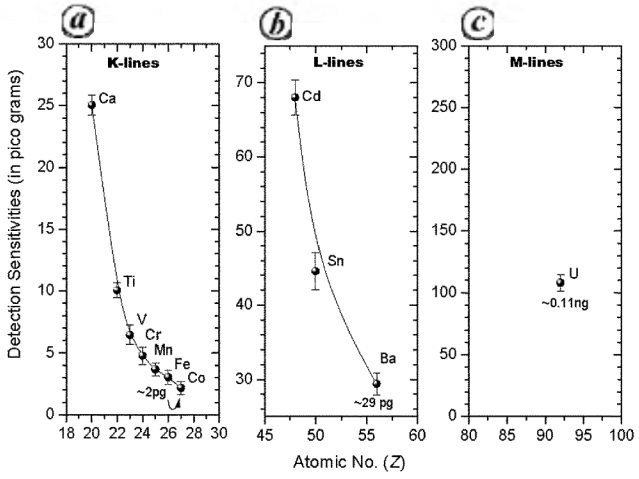

Figure 5. Detection limits determined by TXRF technique applied to residues of aqueous solutions at modest X-ray tube powers. Excitation source: Cu X-ray tube, 30 kV, 40 mA. Analysis time: 1000 s. ***a*–*c*** show the detection limits determined for K-series, L-series and M-series fluorescence lines respectively.

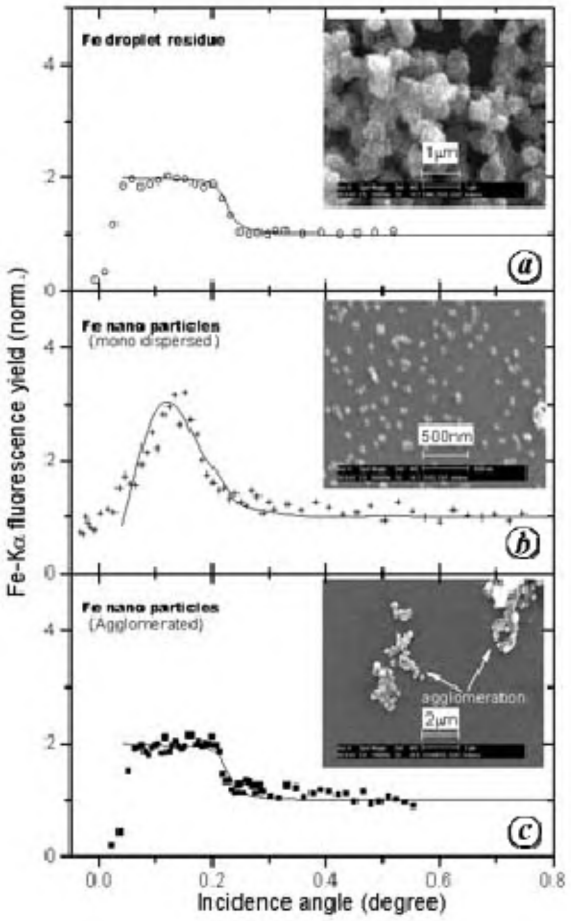

Figure 6. Recorded GIXRF profiles for different forms of Fe particulate matter on top of a Si substrate. ***a***, Droplet residue particles; ***b***, Fe nanoparticles (monodispersed), and ***c***, Fe nanoparticles (agglomerated). Scattered points show measured data, whereas solid lines show fitted GIXRF profiles using the CATGIXRF program. (Insets) SEM image of Fe particles in the respective cases.

we have measured the GIXRF profile for a 20 nm Fe thin film. The computed GIXRF is also shown along with the computed X-ray reflectivity profile. It can be seen that the GIXRF and X-ray reflectivity profiles of a thin film structure are complimentary to each other. The fluorescence intensity is minimum at places where reflectivity is maximum and vice-versa. The Fe-K_α fluorescence intensity increases rapidly as the incidence angle becomes larger than the critical angle of the thin film. For Fe, the critical angle $\phi_c \sim 0.384°$ is at 8.05 keV X-ray energy. The oscillations in the GIXRF profile appear due to interference of the incoming and reflected beams. At higher incidence angles the fluorescence intensity becomes nearly constant as the reflected part of the primary beam decreases abruptly and only incident X-ray beam excites the material. From the best-fit GIXRF result we have obtained the thickness of the Fe film to be ~19.5 ± 0.5 nm, which matches quite well with the value determined using X-ray reflectivity measurements.

Multilayer characterization

Barbee and Warburton[19] have shown that XSW effects can also occur in X-ray multilayer structures as in a perfect crystal[20]. With strong Bragg reflection from a multilayer, a XSW field with periodicity of a multilayer period ($d = \lambda/2\sin\theta_B$), is set up inside the multilayer structure. This XSW field, produced by a multilayer structure, has long been of interest for characterization of intermixing between the layers[21]. In Figure 8, we have shown the GIXRF measurement of a Ni/C periodic multilayer structure [$N = 20$, $\Gamma = 0.47$, $d = 7.0$ nm], wherein the normalized Ni-K_α fluorescence intensity has been plotted along with the reflectivity profile as a function of incidence angle. It

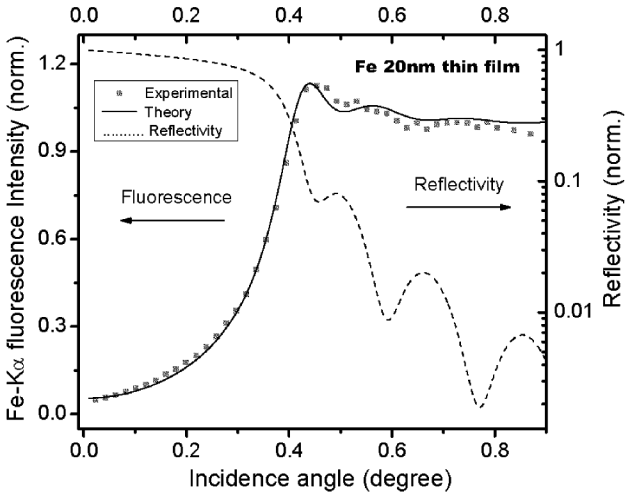

Figure 7. Recorded GIXRF profile of a 20 nm Fe thin film. Scattered points show the experimental data, whereas solid line shows fitted GIXRF profile. Dotted line shows the calculated X-ray reflectivity profile for the film.

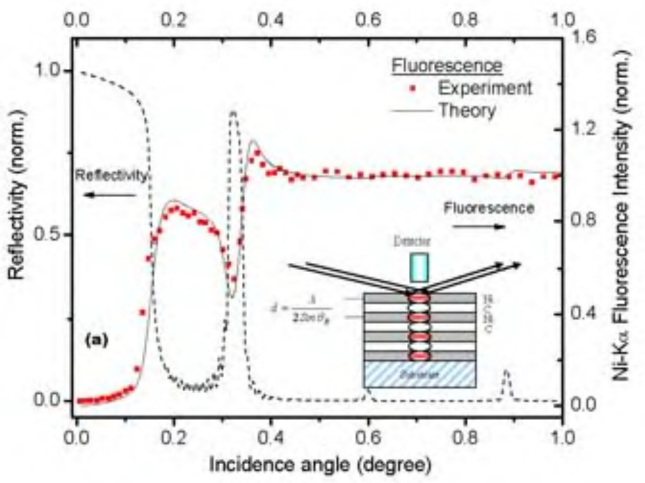

Figure 8. Measured GIXRF profile for a Ni/C multilayer structure. Scattered point and solid line show the experimental and fitted GIXRF profiles respectively. The dotted line shows the calculated X-ray reflectivity profile for the multilayer structure.

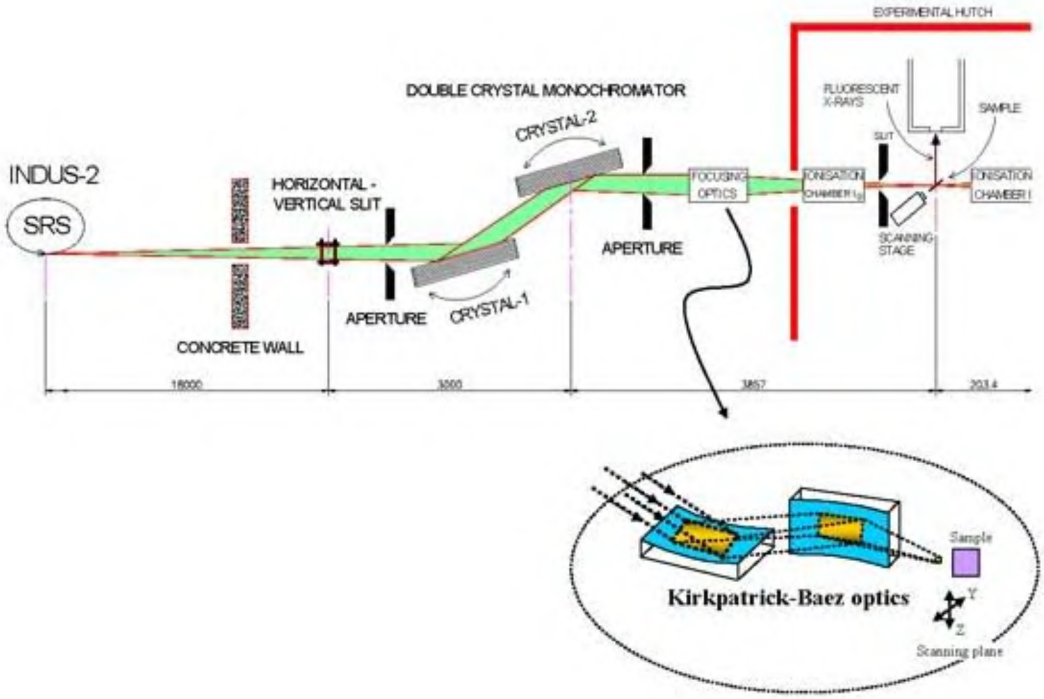

Figure 9. Schematic layout of the microprobe X-ray fluorescence beamline on Indus-2 synchrotron source. The figure is not to scale.

can be seen from Figure 8 that in the vicinity of the first-order Bragg peak, the Ni-K_α fluorescence intensity is modulated in a special way. This modulation in the GIXRF profile arises due to the fact that the XSW antinodes are in low-density layers (i.e. carbon layers) at the low-angle side of the Bragg peak. As incidence angle changes across the Bragg peak region, the antinodes of the standing wave field move inward and finally coincide with high-density layers (Ni layers) at the higher angle side of the Bragg peak. If the interlayer mixing between layers of a multilayer structure is present, the GIXRF profile in the Bragg peak region changes remarkably. The measured GIXRF profile of the Ni/C structure was found to match closely with the calculated profile. The results of XSW characterization of Ni/C multilayer structure have been described elsewhere[12].

XRF activity on Indus-2 synchrotron radiation source

Indus-2 is a 2.5 GeV, third-generation Indian synchrotron source[22] which is being commissioned. As an extension of our XRF activity, an X-ray fluorescence microprobe beamline has been designed and is under construction on the Indus-2 synchrotron source[23]. A schematic of the beamline is given in Figure 9. The microprobe XRF beamline will be installed on a bending magnet source (E_{crit} = 6.21 keV) and will work in the X-ray energy range 4–20 keV. In μ-XRF mode, it would be possible to examine a specimen for spatial distribution of elements. It has been aimed to get an X-ray focal spot of size ~6 μm (H) × 12 μm (V) on the sample position. The expected X-ray photon flux at the sample position in the microprobe mode is ~10^8 photons/s. The maximum analysis area on a specimen will vary from few tens of microns to 25 mm. Apart from elemental mapping, the beamline will offer other modes of XRF characterization, viz. TXRF analysis, normal XRF analysis (in unfocused mode), and chemical speciation or near-edge absorption spectroscopy.

Conclusion

We have described a simple TXRF spectrometer developed in-house and demonstrated its applications. Giving a few examples, we have shown that the TXRF technique with GIXRF and XSW modes of analysis, is a powerful technique for analysing ultra-trace elements and thin-layered materials. GIXRF can provide structural information such as thickness, roughness and density variation. for thin-film structures. The main attraction of GIXRF is that it is an element-specific technique and is highly sensitive to impurity atom positions coinciding with position of maximum energy flow (i.e. XSW antinode), which can be controlled by the incidence angle. The method is especially suitable for nondestructive evaluation of surfaces and interfaces for elemental impurity distribution.

1. Obiajunwa, E. I., Pelemo, D. A., Owolabi, S. A., Fasasi, M. K. and Johnson-Fatokun, F. O., Characterization of heavy metal pollutants of soils and sediments around a crude-oil production terminal using EDXRF *Nucl. Instrum. Methods B*, 2002, **194**, 61–64.

2. Anjos, M. J., Lopes, R. T., Jesus, E. F. O., Assis, J. T., Cesareo, R., Barroso, R. C. and Barradas, C. A. A., Elemental concentration analysis in soil contaminated with recyclable urban garbage by tube-excited energy-dispersive X-ray fluorescence. *Radiat. Phys. Chem.*, 2002, **65**, 495–500.
3. Yip, C. W. Y., Ho, J. P. Y., Nikezic, D. and Yu, K. N., Non-destructive measurement of active-layer thickness of LR 115 SSNTD. *Radiat. Meas.*, 2004, **38**, 1–3.
4. Custódio, P. J., Carvalho, M. L., Nunes, F., Pedroso, S. and Campos, A., Direct analysis of human blood (mothers and newborns) by energy dispersive X-ray fluorescence. *J. Trace Elements Med. Biol.*, 2005, **19**, 151–158.
5. Ekinci, R. and Ekinci, N., An alternative method for the determination of element concentrations in schizophrenic, lung cancer and leukaemia patient bloods. *J. Quant. Spectrosc. Radiat. Transfer*, 2004, **86**, 379–385.
6. Klockenkamper, R., *Total Reflection X-ray Fluorescence Analysis*, John Wiley, NY, 1997, pp. 127–131.
7. Comin, F., Navizet, M., Mangiagalli, P. and Apostolo, G., ID27: an industrial TXRF facility. *ESRF Newsl.*, September 1998, **31**, 28–29.
8. Tiwari, M. K., Gowrisankar, B., Raghuvanshi, V. K., Nandedkar, R. V. and Sawhney, K. J. S., Development of a total reflection X-ray fluorescence spectrometer for ultra-trace element analysis. *Bull. Mater. Sci.*, 2002, **25**, 435–441.
9. Tiwari, M. K., Sawhney, K. J. S., Gowrisankar, B., Raghuvanshi, V. K. and Nandedkar, R. V., A simple and precise TXRF spectrometer: construction and its applications. *Spectrochim. Acta Part B*, 2004, **59**, 1141–1147.
10. Becker, R. S., Golovchenko, J. A. and Patel, J. R., X-ray-standing-wave atom location in heteropolar crystals and the problem of extinction. *Phys. Rev. Lett.*, 1983, **50**, 1858–1861.
11. de Boer, D. K. G., Glancing-incidence X-ray fluorescence of layered materials. *Phys. Rev. B*, 1991, **44**, 498–511.
12. Tiwari, M. K., Naik, S. R., Lodha, G. S. and Nandedkar, R. V., Effect of energy dependence of primary beam divergence on the X-ray standing wave characterization of layered materials. *Anal. Sci.*, 2005, **21**, 757–762.
13. Tiwari, M. K., Modi, M. H., Lodha, G. S., Sinha, A. K., Sawhney, K. J. S. and Nandedkar, R. V., Non-destructive surface characterization of float glass: X-ray reflectivity and grazing incidence X-ray fluorescence analysis. *J. Non-Cryst. Solids*, 2005, **351**, 2341–2347.
14. Rai, S. *et al.*, Surface and interface study of pulsed-laser-deposited off-stoichiometric NiMnSb thin films on Si(100) substrate. *Phys. Rev. B*, 2006, **73**, 035417(1–5).
15. Tiwari, M. K., Ultra-trace elemental analysis using total reflection X-ray fluorescence (TXRF) technique, Ph D thesis, Devi Ahilya University, Indore, 2007.
16. Schwenke, H., Gutschke, R. and Knoth K., Characterization of near surface layers by means of total reflection X-ray fluorescence spectrometry. *Adv. X-ray Anal.*, 1992, **35**, 941–946.
17. Weisbrod, U., Gutschke, R., Knoth, J. and Schwenke, H., X-ray induced fluorescence spectrometry at grazing incidence for quantitative surface and layer analysis. *J. Anal. Chem.*, 1991, **341**, 83–86.
18. Tiwari, M. K., Bhalerao, G. M., Babu, M., Sinha, A. K. and Mukherjee, C., Investigation of metal nanoparticles on a Si surface using an X-ray standing wave field. *J. Appl. Phys.*, 2008, **103**, 054311(1–6).
19. Barbee, T. W. and Warburton, W. K., X-ray standing-wave fluorescence analysis of electrodeposited Tl on clean and oxygen-reconstructed Cu(111). *Mater. Lett.*, 1984, **3**, 17–23.
20. Battermann, B. R., Effect of dynamical diffraction in X-ray fluorescence scattering. *Phys. Rev.*, 1964, **133**, A759–A764.
21. Ghose, S. K. and Dev, B. N., X-ray standing wave and reflectometric characterization of multilayer structures. *Phys. Rev. B*, 2001, **63**, 245409(1–11).
22. Nandedkar, R. V. and Sawhney, K. J. S., Status of Indus-1 and Indus-2 beamlines. *Nucl. Instrum. Methods B*, 2003, **199**, 541–545.
23. Arijit Das, Sinha, A. K. and Nandedkar, R. V., Physics design of micro probe XRF beam line, CAT Internal report, 2005.

ACKNOWLEDGEMENTS. We thank Pragya Tiwari and Mahendra Babu for the SEM investigations of nanoparticles on a Si substrate surface.

Received 15 November 2006; revised accepted 30 July 2007